Geometries and Conformational Processes in Phencyclidine and a Rigid Adamantyl Analogue: Variable-Temperature NMR, X-ray Crystallographic, and Molecular Mechanics Studies

Thomas A. Eaton,† K. N. Houk,*,† Steven F. Watkins,‡ and Frank R. Fronczek‡

Department of Chemistry, University of Pittsburgh, Pittsburgh, Pennsylvania 15260, and Department of Chemistry, Louisiana State University, Baton Rouge, Louisiana 70803. *Received May 21, 1982*

The barriers to rotation of the aryl groups of *m*-nitrophenyladamantylpiperidine and *m*-nitrophenylcyclohexylpiperidine have been studied by variable-temperature NMR spectroscopy. NMR spectra of the free bases and salts of phenyladamantylpiperidine and phenylcyclohexylpiperidine (phencyclidine) and an X-ray crystal structure of the adamantane derivative verify the preferred conformations of these molecules in solution and the solid state. Force-field calculations provide additional information on the energetics of conformational processes in these molecules.

Phencyclidine (1-phenylcyclohexylpiperidine, "angel dust" or PCP) is a potent drug of abuse.[1] This substance

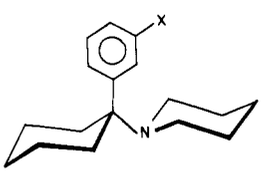

PCP (X=H)
NPCP (X=NO_2)

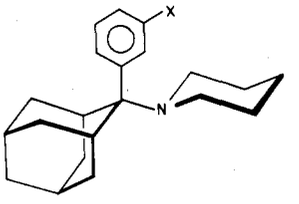

PAP (X = H)
NPAP (X = NO_2)

and a variety of analogues are believed to interfere with cholinergic processes,[2] and an interaction pharmacophore has been developed by Weinstein et al. to rationalize the propensities of these molecules to bind to a common receptor.[3] Central to this model is the postulate that the aromatic ring of PCP is disposed relative to the ammonium group so as to present an electron-rich site to the receptor surface in a fashion similar to that accomplished by the acetyl group of acetylcholine. The conformation shown in Figure 1 is that postulated for PCP at the receptor site.[3a] This is similar to the conformation found in the X-ray crystal structure of phencyclidine hydrochloride,[4] from which it differs by a 180° rotation of the piperidine ring about the exocyclic C–N bond. Rigid analogues of PCP, having an adamantyl group in place of the cyclohexyl moiety, have been synthesized, and are found to be more potent in vitro muscarinic antagonists than PCP, although inactive in vivo due to limited solubility.[5] Increased activity at the receptor site was predicted to result from the greater rigidity of the system, which enforces the correct conformation for ideal interaction with the receptor.

However, a drug does not necessarily bind to its receptor via its most stable conformation. Any energetically accessible conformation may be involved in binding. This makes the energetics of the conformational processes of great interest, since these quantities allow certain high-energy conformers to be excluded from consideration as candidates for complexation with the receptor. This study was undertaken in order to determine the preferred conformations of the aromatic and piperidine moieties of 2-phenyl-2-piperidinoadamantane (PAP) in solution and to determine the energetics of conformational changes in this molecule and in PCP itself. These goals were accomplished through analysis of ^1H and ^{13}C variable-temperature nuclear magnetic resonance (NMR) spectra of the parent molecules, the *m*-nitro derivatives, NPAP and NPCP, and the hydrochloride salts of these molecules. The preferred solution conformation has also been shown to be that found in the crystalline state by X-ray crystallographic studies.

In a study related to ours, Cone et al. synthesized analogues of PCP designed to have different distances between the aromatic ring and the piperidine nitrogen.[3b] These authors did not consider, however, the possibility that the preferred conformation of the phenyl group with respect to the nitrogen, rather than the distance between these sites, could be the dominant factor in influencing activity.

The conformational processes in phencylidine are summarized in Figure 2. Phenyl rotation alters the direction in which the electron-rich face of the aromatic ring extends in space relative to the amine group, or ammonium group of the protonated species. Although the conformation of the phenyl shown in Figure 1 is that found in the crystal structure of PCP·HCl,[4] more or less free rotation of this phenyl might be expected in solution, unless the repulsions between the phenyl ortho hydrogens and the 3-axial protons of the cyclohexane are large in rotated conformations. Piperidine rotation can give three staggered conformations, two of which are enantiomeric. Piperidine nitrogen inversion can produce the same conformation as a 180° rotation of the piperidine. Cyclohexyl ring inversion exchanges phenyl and piperidine positions. This latter process has been investigated previously by ^1H and ^{13}C NMR studies.[6,7] Although the phenyl-axial conformation is found to be preferred in PCP, the difference in energy between the two chair cyclohexane conformations is found to be small.

In the following sections, we present first the evidence for solution conformations and then compare these with

† University of Pittsburgh.
‡ Louisiana State University.

(1) Shulgin, A. T.; MacLean, D. E. *Clin. Toxicol.* **1976**, *9*, 553. Peterson, R. C.; Stillman, R. C. *NIDA Res. Monogr.* **1978**, *21*, 1.
(2) Maayani, S.; Weinstein, H.; Cohen, S.; Sokolovsky, M. *Proc. Natl. Acad. Sci. U.S.A.* **1973**, *70*, 3103.
(3) (a) Weinstein, H.; Maayani, S.; Srebrenik, S.; Cohen, S.; Sokolovsky, M.; *Mol. Pharmacol.* **1973**, *9*, 820. (b) McQuinn, R. L.; Cone, E. J.; Shannon, H. E.; Su, Tsung-Ping *J. Med. Chem.* **1981**, *24*, 1429.
(4) Argos, P.; Barr, R. E.; Weber, A. H., *Acta Crystallogr., Sect. B* **1970**, *B26*, 53. See also Briard, P.; Roques, R.; Kamenka, J. M.; Geneste, P.; Declercq, J. P.; Germain, G. *Cryst. Struct. Commun.* **1982**, *11*, 231.
(5) Gabrielevitz, A.; Kloog, Y.; Kalir, A.; Balderman, D.; Sokolovsky, M. *Life Sci.* **1980**, *26*, 89. Geneste, P.; Kamenka, J. M.; Herrmann, P.; Goudal, R.; Trouiller, G. *Eur. J. Med. Chem.-Chim. Ther.* **1979**, *14*, 301.
(6) (a) Mousseron, M.; Bessiere, J.-M.; Geneste, P.; Kamenka, J.-M.; Marty, C. *Bull. Soc. Chim. Fr.* **1968**, 3803. (b) Mousseron, M.; Kamenka, J.-M,; Darvich, M. R. *Ibid.* **1970**, 1435.
(7) (a) Geneste, P.; Kamenka, J. M., *Org. Magn. Reson.* **1975**, *2*, 579. (b) Geneste, P.; Kamenka, J. M.; Ung, M. S. N.; Herrman, P.; Goudal, R.; Troullier, G. *Eur. J. Med. Chem.* **1979**, *14*, 301. (c) Brine, G. A.; Williams, E. E.; Boldt, K. G.; Carroll, F. I., *J. Heterocycl. Chem.* **1979**, *16*, 1425.

0022-2623/83/1826-0479$01.50/0

Table I. Assignments for ^{1}H NMR Spectra of Compounds Studied Here and Models

	PAP	PAP·HCl	NPAP	NPAP·HCl	PCP (−60 °C)	PCP·HCl	NPCP (−60 °C)	NPCP·HCl	piperidine	2-aminoadamantane
A	1.15	2.63	1.10	2.70	1.55	2.53	1.55	2.47	2.80	
B	2.92	3.69	2.98	3.79	3.251	3.72	3.23	3.78	2.80	
C	1.50	2.34	1.52	2.32	1.55	2.12	1.55	2.18	1.53	
D	1.50	1.68	1.52	1.58	1.55	1.78	1.55	1.88	1.53	
E	0.86	1.04	0.89	1.11	0.89	1.15	0.88	1.11	1.53	
F	1.65	1.80	1.72	1.83	1.55	1.78	1.29	1.88	1.53	
G	2.75	3.09	2.76	3.18	2.90	2.85	2.85	2.93		1.8
H					1.55	2.64	1.75	2.64		
I	1.50	1.99	1.52	2.00	1.11	1.15	1.08	1.11		1.77
J	1.65	1.80	1.72	1.83	1.55	1.78	1.55	1.88		1.77
K	1.50	1.80	1.52	1.83	1.30	1.53	1.29	1.60		1.8
L					1.30	1.45	1.29	1.45		
M	2.50	2.76	2.45	2.85						1.95
N	1.65	1.80	1.52	1.83						1.53
O	1.90	2.23	1.93	2.23						1.8
P	1.65	1.80	1.72	1.83						1.77

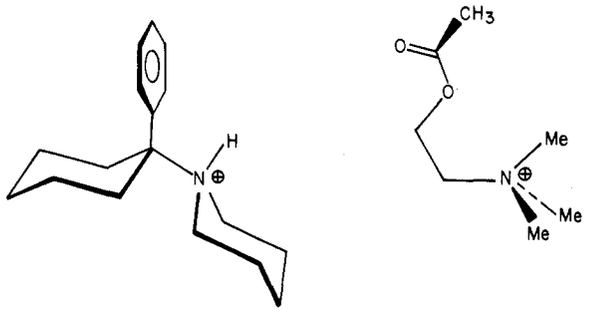

Figure 1. Postulated conformations of phencyclidine and acetylcholine for receptor binding.

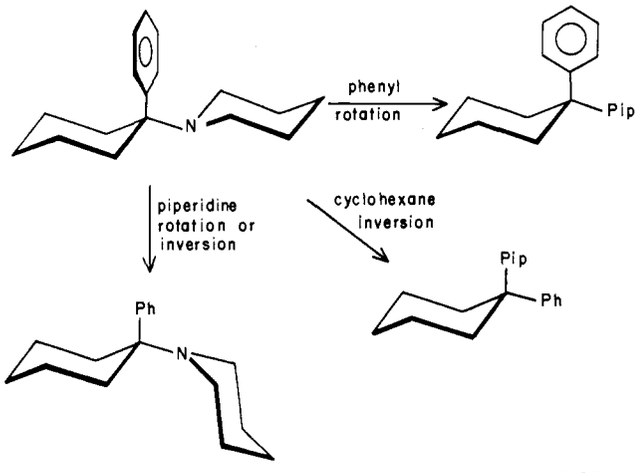

Figure 2. Some limiting conformational processes in PCP.

crystallographic structures. We then describe the dynamic ^{1}H and ^{13}C NMR studies of conformational processes. Finally, these are compared with partial potential energy surfaces calculated by molecular mechanics methods.[8]

NMR Spectral Assignments. NMR spectra were recorded on a Bruker WH-300 300-MHz nuclear magnetic resonance spectrometer at the University of Pittsburgh. Figure 3 shows room-temperature 300-MHz proton spectra of PAP, the corresponding hydrochloride salt PAP·HCl, and the *m*-nitro derivative NPAP. In each of the spectra, resonances are lettered in accord with the labeling scheme shown. The unlabeled positions are symmetry equivalent A′, etc., protons. The assignments were made by comparisons to spectra of model compounds, chemical-shift

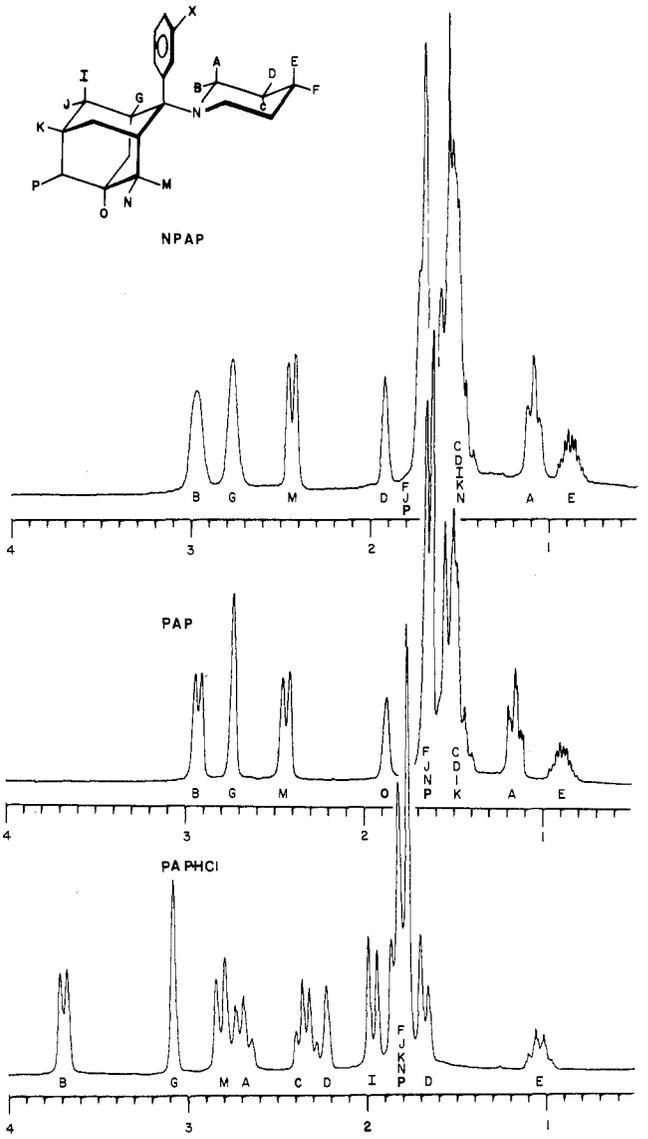

Figure 3. 300-MHz ^{1}H NMR spectra of NPAP, PAP, and PAP·HCl.

behavior on protonation, alterations of the spectra at different temperatures, analyses of coupling patterns, and decoupling experiments. For PAP, a 600-MHz spectrum allowed assignments for regions not resolved in the 300-MHz spectra. Table I contains assignments made for the proton spectra throughout the series of molecules and gives

(8) Review: Allinger, N. L. *Adv. Phys. Org. Chem.* **1976**, *13*, 1. Allinger, N. L., *J. Am. Chem. Soc.* **1977**, *99*, 8127. Allinger, N. L.; Yuh, Y. *CPE* **1980**, *12*, 395.

Table II. ^{13}C NMR Chemical Shifts of PAP, NPAP, and Models

carbon	adamantane	2-amino-adamantane	2-phenyl-adamantane	predicted for PAP[a]	PAP	NPAP
1	28.5	35.5	31.1	37.8	34.0	33.7
2	37.8	55.8	46.8	64.4	64.4	64.7
3	28.5	35.5	31.1	37.8	34.0	33.7
4	37.8	31.2	39.2	32.3	32.3	31.9
5	28.5	27.9	27.8	27.1	27.6	27.2
6	37.8	38.6	37.9	38.3	38.3	38.0
7	28.5	28.4	28.0	27.6	27.7	27.4
8	37.8	38.2	31.9	31.8	30.4	30.3
9	37.8	31.2	39.2	32.2	32.3	31.9
10	37.8	38.2	31.9	31.8	30.4	30.3
11					45.2	45.1
12					27.3	27.0
13					25.4	25.2
14					27.3	27.0
15					45.2	45.1
16					137.6	139.6
17					127.2	121.1
18					126.8	147.7
19					125.6	120.9
20					126.8	128.3
21					127.2	132.9

[a] Calculated for each position as: δ (predicted) = δ (adamantane) + SCS (2-aminoadamantane) + SCS (2-phenyladamantane), where SCS (2-aminoadamantane) = δ (2-aminoadamantane) − δ (adamantane) and SCS (2-phenyladamantane) = δ (2-phenyladamantane) − δ (adamantane).

chemical shifts for two model compounds, piperidine and 2-aminoadamantane.[9]

Assignments for PAP can be made by comparison with model compounds, with the following exceptions. There is a high-field resonance at 0.89 ppm in the spectra of PAP, which is assigned to *E*, the axial hydrogen at C4 of the piperidine ring. This assignment is supported by the doublet of triplet of triplet pattern of this resonance. The anomalously high-field position of this resonance is compatible only with a conformation having this hydrogen in the shielding zone of the aromatic ring. The axial hydrogens, A, at C2 of the piperidine ring are shifted upfield by 1.77 ppm from resonances of their equatorial counterparts, B. Chemical-shift differences of 0.93 ppm between axial and equatorial protons α to nitrogen are generally observed for saturated nitrogen heterocycles such as quinolizidine.[10]

The unusually large difference in chemical shifts (1.77 ppm) of A and B, also found for NPAP, may be attributed in part to the usual axial–equatorial C2 effect.[10] This indicates that nitrogen inversion is slow on the NMR time scale, since rapid inversion, accompanied by rotation, would make A and B equivalent. The chemical-shift difference is accentuated by the location of A in the shielding zone of the phenyl group. This chemical-shift difference is still over 1 ppm for the hydrochloride salts of PAP and PAP·HCl, indicating that these molecules also exist with essentially a single piperidine conformation in solution.

Several resonances due to protons on the adamantyl moiety are also anomalous when compared to the model compound, 2-aminoadamantane. The methine protons labeled G are adjacent to the quaternary center and are shifted downfield by 0.95 ppm. The axial methylene protons, I, in the shielding region of the benzene ring appear upfield by 0.27 ppm, while those labeled M are deshielded by the phenyl ring and are shifted downfield by 0.55 ppm. Also, methine proton K is shifted upfield by 0.3 ppm; the other methine proton, O, is shifted downfield by 0.1 ppm.

Conversion from free base to hydrochloride shifts peaks of hydrogens α to nitrogen downfield by 1.48 ppm for axial protons, A, and 0.77 ppm for equatorial counterparts, B. Axial protons, C, one carbon removed are also shifted downfield by 0.84 ppm. Assignments of A and C in the hydrochloride salt are supported by decoupling experiments, which show mutual coupling as well as coupling to E. Other peaks are shifted downfield by 0.2–0.3 ppm by protonation of the amine.

Figure 4 shows the low-temperature 300-MHz spectra of PCP and PCP·HCl. There is virtually peak for peak correspondence between the spectra of the rigid molecules and PCP or NPCP, except, of course, where extra protons are present in PCP. Three peaks, due to E, A, and B, define the preferred piperidine conformation as equivalent to that in the rigid analogues and observed in the solid state (see later). Most significant is the upfield position of E, which is overlapped by resonances due to protons I in the phencyclidines and indicates shielding by the phenyl ring. The 1.19-ppm chemical-shift difference between axial and equatorial protons A and B again implies that there is a highly preferred conformation of both the phenyl and piperidine moieties. In addition, the conformation of the cyclohexane ring is inferred, particularly from the upfield shift of resonance I, to be that with the phenyl axial and piperidine equatorial, as noted in previous studies.[6,7]

Low-temperature spectra of phencyclidine free bases are similar to those of the room-temperature spectra of the rigid analogues. Nitrogen inversion appears frozen in the −60 to −65 °C spectra of PCP and NPCP, where piperidine axial–equatorial chemical-shift differences of 1.70 and 1.68 ppm are observed.

As noted earlier for the hydrochloride salts, little conformational flexibility is indicated in the cyclohexyl region. Axial–equatorial chemical-shift differences of 0.44 and 0.47 ppm are observed in the low-temperature spectra for the C3, C5 cyclohexyl protons of PCP and its NPCP derivative. About 0.15 to 0.20 ppm of this difference is due to shielding by the aromatic ring, as indicated by the axial–equatorial chemical-shift difference in the adamantyl derivatives.

(9) Van Deursen, F. W.; Korver, P. K. *Tetrahedron Lett.* **1967**, 3923.

(10) Hanlow, H. P.; Okuda, S. *Tetrahedron Lett.* **1964**, *2*, 553. Vierhapper, F. W.; Eliel, E. L. *J. Org. Chem.* **1979**, *44*, 1081.

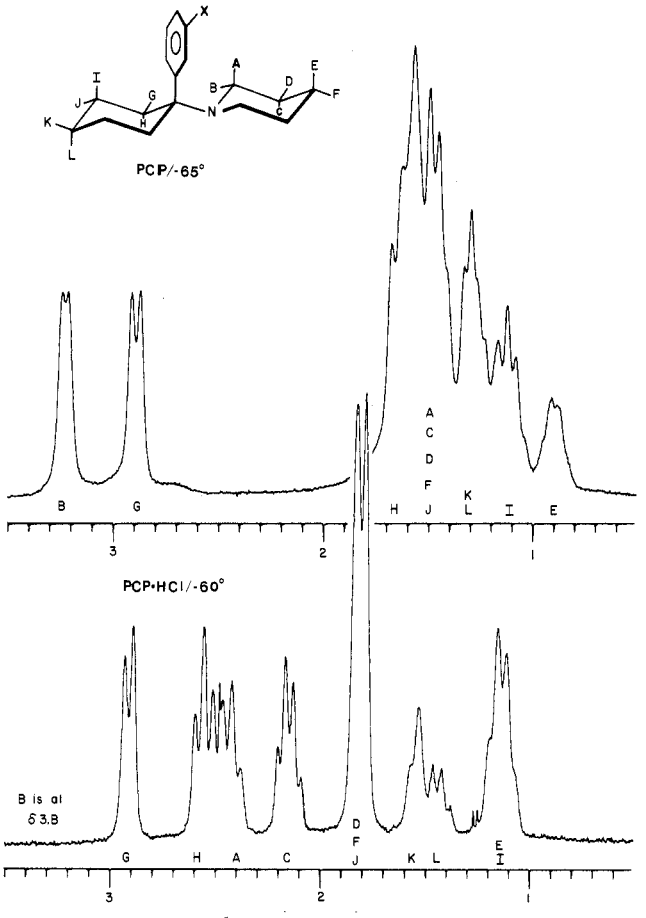

Figure 4. 300-MHz ^1H NMR spectra of PCP at −65 °C and PCP·HCl at −60 °C.

^{13}C NMR Spectra of PAP and NPAP. Natural abundance ^{13}C spectra were recorded at 75.46 MHz in $CDCl_3$ with broad-band proton decoupling. The spectrum of NPAP is shown in Figure 5, and the data are summarized in Table II, along with those used for assignments of the carbon resonances. The positions of adamantyl ^{13}C resonances in PAP and NPAP were predicted from the substituent chemical shift (SCS) values calculated by a comparison of the 2-amino- and 2-phenyladamantane spectra to that of adamantane. Piperidine resonances were assigned by analogy to PCP,[11a] while aromatic positions were assigned by adding SCS for the nitro group[11b] to PCP phenyl resonances.

The Solution Conformation of PAP and PCP. The NMR spectral evidence indicates that the phenyl conformation given in the drawing shown above is preferred for both PAP and PCP. The data also agree with earlier ^1H and ^{13}C NMR evidence that piperidine preferentially occupies an equatorial position in PCP.[6,7] Upfield shifts of the axial protons α to N and of the single piperidine methylene proton, E, indicate that this ring does not have appreciable populations of conformations other than that shown in the drawing above. The upfield shifts are also indicative of the preferred conformation of phenyl, while partial resolution of the adamantyl peaks in NPAP indicate the aryl group rotates slowly. Hydrochloride salt spectra show rigidity in both the cyclohexyl and piperidine portions of PCP and NPCP, indicated by clean separation of axial and equatorial protons.

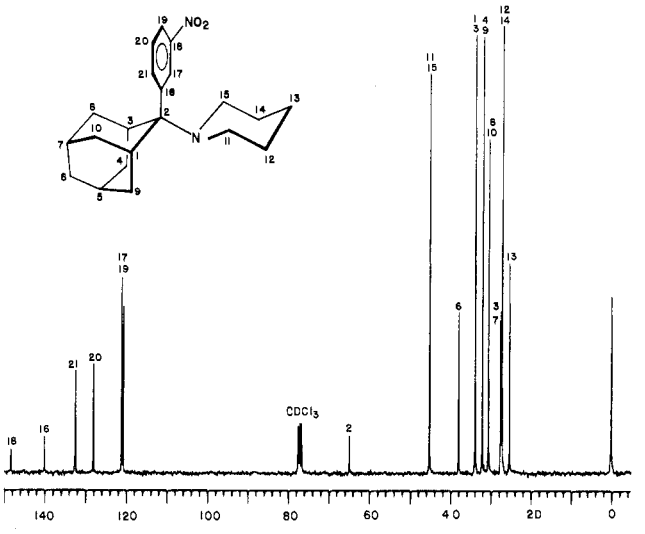

Figure 5. Proton-decoupled 75.46-MHz ^{13}C spectra of NPAP in ($CDCl_3$).

X-ray Crystal Structure of PAP. Crystal Data. PAP, $C_{21}H_{29}N$, has M_r = 295.5, monoclinic space group $P2_1/n$, a = 6.433 (1), b = 15.888 (2), c = 16.320 (3) Å, β = 98.66 (2)°, Z = 4, d_c = 1.190 g cm^{-3}, μ (Cu $K\alpha$) = 5.148 cm^{-1}, R = 0.055 for 1503 observed data.

Intensity data were obtained from a colorless crystal of dimensions 0.20 × 0.24 × 0.32 mm mounted in random orientation on an Enraf-Nonius CAD4 automatic diffractometer at Louisiana State University. One quadrant of data having $2° < \theta < 60°$ was measured using graphite-monochromatized Cu $K\alpha$ radiation (λ = 1.54184 Å). The $\omega - 2\theta$ scans were made at rates varying from 0.45 to 10.0 deg min^{-1} in order to measure all significant data with approximately equal precision. Reflections having $I_{obsd} > \delta$ (I_{obsd}) in a 10.0 deg min^{-1} prescan were flagged as unobserved and not scanned slowly. No significant decrease in the intensities of periodically remeasured standard reflections was noted. A total of 2449 independent data was measured in this manner, of which 1503 had $F_{obsd} > 3\delta(F_{obsd})$ and were used in further calculations. Data were corrected for background, Lorentz, and polarization effects. Absorption corrections were made by an empirical procedure based on ψ scans made for reflections near ψ = 90°. The minimum relative transmission factor was 0.8803.

The space group was determined from systematic absences oko with k odd and hol with $h + l$ odd. The structure was solved by routine application of multiple solution direct methods employing MULTAN 78[14] and refined by full-matrix least squares by using the Enraf–Nonius structure determination package.[15] Refinement was based upon F with unit weights, treating non-hydrogen atoms anisotropically. Hydrogen atoms were located from difference maps as peaks of density 0.24–0.53 eA^3 and were included as fixed contributions with B = 5.0. A final

(11) (a) Bailey, K.; Legault, D. *Anal. Chim. Acta* **1980**, *113*, 375. (b) Levy, G. C.; Nelson, G. L. "Carbon-13 NMR for Organic Chemists"; Wiley: New York, 1972; p 81.
(12) Duddeck, H.; Hollowood, F.; Karim, A.; McKervey, M. A. *J. Chem. Soc., Perkin Trans. 2* **1979**, 360.
(13) Maciel, G. E.; Dorn, H. C.; Greene, R. L.; Kleschick, W. A.; Peterson, Jr., M. R.; Wahl, Jr., G. H. *Org. Magn. Reson.* **1974**, *6*, 178.
(14) Frenz, B. A.; Okaya, Y. "Enraf-Nonius Structure determination Package"; Enraf-Nonius: Delft, Holland; 1980.
(15) Main, P.; Hall, S. E.; Lessinger, L.; Germain, G.; Delcercq, J. P.; Woolfson, M. M. "MULTAN, A System of Computer Programs for the Automatic Solution of Crystal Structures From X-ray Diffraction Data"; Universities of York and Louvain: England and Belgium, respectively; 1978.

Table III. Positional and Thermal Parameters and Their Estimated Standard Deviations for PAP

atom	x	y	z	B_{11}	B_{22}	B_{33}	B_{12}	B_{13}	B_{23}
N1	0.1353 (7)	0.7832 (3)	0.8429 (3)	0.012 (1)	0.0032 (2)	0.0027 (2)	−0.0004 (9)	0.0023 (7)	−0.0012 (4)
C1	0.2195 (8)	0.6503 (4)	0.7759 (3)	0.010 (1)	0.0027 (3)	0.0029 (2)	0.000 (1)	0.0016 (9)	0.0002 (4)
C2	0.1576 (9)	0.5887 (4)	0.7042 (4)	0.015 (1)	0.0029 (3)	0.0035 (2)	0.002 (1)	0.0043 (10)	−0.0005 (5)
C3	−0.0672 (9)	0.5560 (4)	0.7063 (4)	0.018 (2)	0.0030 (3)	0.0033 (3)	−0.002 (1)	0.0012 (10)	−0.0010 (5)
C4	−0.0757 (10)	0.5112 (4)	0.7884 (4)	0.022 (2)	0.0032 (3)	0.0045 (3)	−0.002 (1)	0.0029 (12)	0.0011 (5)
C5	−0.0137 (9)	0.5712 (4)	0.8601 (4)	0.020 (2)	0.0037 (3)	0.0032 (3)	−0.003 (1)	0.0037 (10)	0.0018 (5)
C6	0.2137 (9)	0.6041 (4)	0.8577 (4)	0.014 (1)	0.0038 (3)	0.0033 (2)	0.002 (1)	0.0001 (10)	0.0011 (5)
C7	−0.2128 (8)	0.6324 (4)	0.6980 (3)	0.013 (1)	0.0036 (3)	0.0027 (2)	−0.003 (1)	0.0018 (9)	−0.0008 (5)
C8	−0.1519 (8)	0.6938 (4)	0.7704 (3)	0.008 (1)	0.0036 (3)	0.0025 (2)	−0 000 (1)	0.0025 (8)	0.0001 (4)
C9	−0.1597 (9)	0.6476 (4)	0.8523 (3)	0.014 (1)	0.0039 (3)	0.0028 (2)	−0.003 (1)	0.0035 (9)	0.0007 (5)
C10	0.0776 (8)	0.7295 (4)	0.7687 (3)	0.009 (1)	0.0027 (2)	0.0022 (2)	−0.000 (1)	0.0022 (8)	−0.0004 (4)
C11	0.0870 (8)	0.7785 (4)	0.6899 (3)	0.012 (1)	0.0032 (3)	0.0022 (2)	0.001 (1)	0.0026 (8)	0.0001 (4)
C12	0.2744 (8)	0.7831 (4)	0.6535 (4)	0.013 (1)	0.0047 (3)	0.0029 (2)	−0.001 (1)	0.0028 (9)	0.0005 (5)
C13	0.2851 (9)	0.8308 (5)	0.5843 (4)	0.020 (2)	0.0065 (4)	0.0027 (2)	−0.003 (1)	0.0057 (10)	0.0014 (6)
C14	0.1244 (10)	0.8834 (4)	0.5509 (4)	0.032 (2)	0.0044 (3)	0.0022 (2)	−0.004 (1)	0.0041 (11)	0.0010 (5)
C15	−0.0629 (10)	0.8812 (5)	0.5862 (4)	0.025 (2)	0.0048 (3)	0.0028 (2)	0.005 (1)	0.0013 (11)	0.0015 (5)
C16	−0.0735 (9)	0.8326 (4)	0.6552 (4)	0.019 (2)	0.0035 (3)	0.0031 (2)	0.003 (1)	0.0050 (10)	0.0011 (5)
C17	0.3554 (9)	0.8111 (4)	0.8599 (4)	0.011 (1)	0.0050 (3)	0.0040 (3)	−0.003 (1)	0.0023 (10)	−0.0027 (5)
C18	0.4120 (10)	0.8470 (5)	0.9441 (4)	0.018 (2)	0.0057 (4)	0.0039 (3)	−0.004 (1)	0.0001 (11)	−0.0028 (6)
C19	0.2715 (11)	0.9181 (4)	0.9618 (4)	0.030 (2)	0.0042 (3)	0.0026 (2)	−0.005 (1)	0.0010 (12)	−0.0017 (5)
C20	0.0432 (10)	0.8918 (5)	0.9386 (4)	0.023 (2)	0.0054 (4)	0.0043 (3)	0.002 (1)	0.0040 (12)	−0.0040 (6)
C21	−0.0004 (9)	0.8544 (4)	0.8542 (4)	0.018 (2)	0.0040 (3)	0.0038 (3)	0.002 (1)	0.0019 (11)	−0.0027 (5)

[a] The form of the anisotropic thermal parameter is as follows: $\exp(B_{11}H^2 + B_{22}K^2 + B_{33}L^2 + B_{12}HK + B_{13}HL + B_{13}KL)$.

Table IV. Assigned Hydrogen Atom Parameters for PAP

atom	x	y	z	B, Å^2	atom	x	y	z	B, Å^2
H22	0.3606	0.6705	0.7729	5.0	H37	0.4093	0.8287	0.5584	5.0
H23	0.2633	0.5415	0.7090	5.0	H38	0.1387	0.9212	0.5051	5.0
H24	0.1645	0.6154	0.6521	5.0	H39	−0.1847	0.9137	0.5613	5.0
H25	−0.1116	0.5165	0.6613	5.0	H40	−0.1992	0.8356	0.6813	5.0
H26	0.0158	0.4631	0.7944	5.0	H41	0.3792	0.8531	0.8192	5.0
H27	−0.2171	0.4902	0.7907	5.0	H42	0.4460	0.7642	0.8527	5.0
H28	−0.0234	0.5405	0.9106	5.0	H43	0.5556	0.8666	0.9623	5.0
H29	0.2538	0.6414	0.9038	5.0	H44	0.4017	0.0039	0.9846	5.0
H30	0.3107	0.5577	0.8636	5.0	H45	0.2970	0.9666	0.9276	5.0
H31	−0.3554	0.6142	0.6969	5.0	H46	0.3013	0.9360	0.0181	5.0
H32	−0.2038	0.6605	0.6467	5.0	H47	−0.0480	0.9390	0.9441	5.0
H33	−0.2498	0.7402	0.7656	5.0	H48	0.0131	0.8499	0.9787	5.0
H34	−0.1175	0.6852	0.8974	5.0	H49	0.0177	0.8983	0.8141	5.0
H35	−0.3012	0.6300	0.8545	5.0	H50	−0.1461	0.8373	0.8422	5.0
H36	0.3952	0.7501	0.6775	5.0					

difference Fourier yielded no residuals greater than 0.24 eÅ^{-3}.

Position parameters are given in Tables III and IV, while bond lengths and bond angles are listed in Table V. Some relevant torsional angles are given in Table VI.

The ORTEP drawing of the X-ray structure of PAP is shown in Figure 6. It is clear that the preferred conformation of PAP is the same as that determined for PCP and PAP in solution.

A referee has pointed out the unusual distortion of the phenyl group on PAP. In particular, the C12–C11–C16 angle is 114.8°, and the ring is distorted so that the dihedral angles are all ±5° and alternate in sign around the ring. These distortions are most likely due to the close approach (2.0 Å) of the ortho hydrogens on the aromatic ring to the hydrogens on C-1 and C-8 (numbering as in Figure 6). Phenyl rotation would relieve these close contacts but would introduce more severe repulsions of the ortho hydrogens with the axial hydrogens at C-2 or C-7 of the adamantane ring and at C-17 and C-21 of the piperidine ring.

Some of the interatomic distances relevant to our discussion in PAP and in the X-ray structure of the HCl salt of PCP[4] are compared in Figure 7. Of particular note, the 1,3-diaxial distances between the phenyl groups and the axial hydrogens are larger for PCP than for PAP, so that rotation of the phenyl group in PCP should be easier than that in PAP.

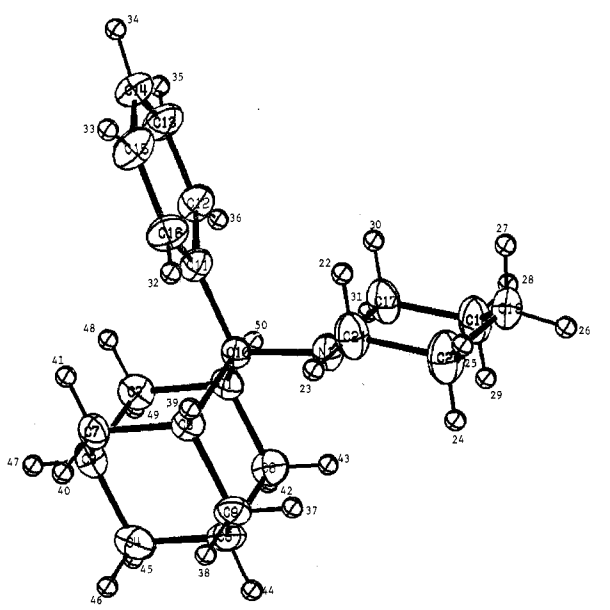

Figure 6. ORTEP drawing of the solid-state structures of PAP and PCP·HCl.[4]

MM2 Calculations. The conclusions from X-ray and solution data are supported by MM2 calculations.[8] Calculations were made by using X-ray crystallographic co-

Table V. Bond Lengths and Bond Angles in NPAP

atoms	distance, Å	atoms	distance, Å
C1-C2	1.531 (7)	C10-N1	1.482 (6)
C1-C6	1.528 (7)	C11-C12	1.424 (6)
C1-C10	1.549 (6)	C12-C13	1.372 (7)
C2-C3	1.541 (6)	C13-C14	1.377 (7)
C3-C4	1.524 (7)	C14-C15	1.412 (7)
C3-C7	1.527 (7)	C15-C16	1.377 (7)
C4-C5	1.515 (8)	C16-C11	1.396 (6)
C5-C6	1.560 (7)	C17-N1	1.470 (6)
C5-C9	1.529 (7)	C17-C18	1.481 (7)
C7-C8	1.537 (6)	C18-C19	1.502 (8)
C8-C9	1.534 (6)	C19-C20	1.520 (7)
C8-C10	1.586 (6)	C20-C21	1.488 (7)
C10-C11	1.511 (6)	C21-N1	1.458 (6)
C2-C1-C6	108.9 (4)	N1-C10-C8	108.1 (4)
C2-C1-C10	112.3 (4)	N1-C10-C11	111.2 (4)
C6-C1-C10	111.4 (4)	C8-C10-C11	110.8 (4)
C1-C2-C3	109.6 (4)	C10-C11-C12	121.7 (4)
C2-C3-C4	109.6 (4)	C10-C11-C16	122.7 (4)
C2-C3-C7	107.2 (4)	C12-C11-C16	114.8 (4)
C4-C3-C7	110.2 (4)	C11-C12-C13	121.6 (5)
C3-C4-C5	110.2 (4)	C12-C13-C14	122.2 (5)
C4-C5-C6	109.3 (4)	C13-C14-C15	117.4 (5)
C4-C5-C9	110.4 (4)	C14-C15-C16	119.9 (5)
C6-C5-C9	107.4 (4)	C11-C16-C15	123.6 (5)
C1-C6-C5	109.2 (4)	C10-N1-C17	116.4 (4)
C3-C7-C8	110.8 (4)	C10-N1-C21	118.0 (4)
C7-C8-C9	109.1 (4)	C17-N1-C21	108.7 (4)
C7-C8-C10	110.1 (4)	N1-C17-C18	112.8 (4)
C9-C8-C10	109.8 (4)	C17-C18-C19	113.4 (5)
C5-C9-C8	110.6 (4)	C18-C19-C20	109.4 (5)
C1-C10-N1	109.5 (4)	C19- C20-C21	112.4 (5)
C1-C10-C8	104.4 (4)	C20-C21-N1	113.3 (5)
C1-C10-C11	112.6 (4)		

Table VI. Selected Torsion Angles for PAP[a]

atom 1	atom 2	atom 3	atom 4	angle, deg
		Phenyl Ring		
C11	C12	C13	C14	6.8
C12	C13	C14	C15	-5.7
C13	C14	C15	C16	4.9
C14	C15	C16	C11	-5.4
C15	C16	C11	C12	6.0
C16	C11	C12	C13	-6.5
		Piperidine Ring		
N1	C17	C18	C19	-55.4
C17	C18	C19	C20	49.5
C18	C19	C20	C21	-49.2
C19	C20	C21	N1	55.6
C20	C21	N1	C17	-57.8
C21	N1	C17	C18	57.2

[a] esd's are 0.6-0.7°.

ordinates as input, and various conformations were optimized by using symmetry restrictions, oriented so that rotation was driven about the z axis. The phenyl group has standard bond lengths and bond angles, and its motion was restricted, since MM2 contains no explicit π interactions. Symmetry restrictions were then removed, and the dihedral driver was applied by using 10° intervals. Structures were optimized at each interval, excluding the phenyl ring parameters, which were fixed.

The minimum energy conformation for PAP is predicted to be that with the phenyl group parallel to a line joining the axial piperidine, or adamantyl, protons. A second very shallow (0.75 kcal) minimum exists with the phenyl group perpendicular to this line, lying 21.3 kcal/mol above the global minimum. The activation barrier for phenyl rotation is calculated to be 22 kcal/mol, some 7–9 kcal/mol above that determined experimentally, as described in the next section. Nonetheless, it is of the right order of magnitude, since the "torsional driver" technique used for these calculations is known to give barriers that are somewhat too high.[16] Furthermore, the phenyl group is rigid, and not optimized, in these calculations.

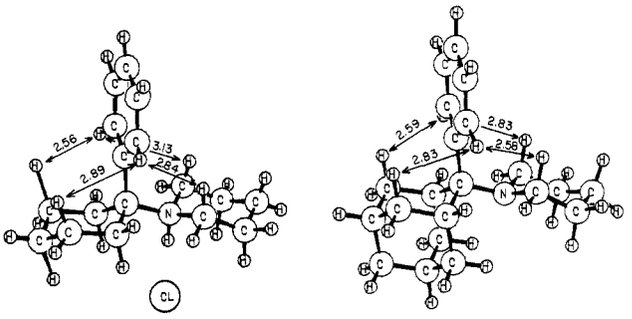

Figure 7. Some interatomic distances in PCP·HCl and PAP.

The major source of this 22 kcal/mol barrier, amounting to 9 kcal, is the van der Waals interactions between nonbonded hydrogen atoms. These are due mainly to interactions between axial adamantyl and piperidine protons and phenyl ortho protons. These four interactions constitute 8 kcal/mol of the barrier.

For PCP, MM2 shows two minima with approximately the same energies, that with the phenyl equatorial lying 0.2 kcal/mol lower than that with phenyl axial, in contrast to NMR evidence, which favors an axial phenyl group.[7a,c] Once again, this discrepancy is likely due to our crude model for the phenyl group. For the axial phenyl conformer, the structure with the phenyl group "parallel" (as in the X-ray crystal structure) is the only minimum, with a rotational barrier of 13.3 kcal/mol. For the phenyl-equatorial conformation, the barrier is even lower, 7.4 kcal/mol, with a second shallow minimum (0.7 kcal/mol) with the phenyl group "perpendicular". Assuming that these barriers are again overestimated, it is reasonable that we were unable to freeze out phenyl rotamers of NPCP and its NPCP·HCl at a low temperature (see below).

The major energy change in the less rigid PCP molecule is due to bending, but van der Waals interactions are again important. Although overall nonvicinal van der Waals interaction energies change by 3.3 kcal/mol, interactions between axial phenyl ortho protons and axial cyclohexyl and piperidine protons increase by 5 kcal/mol. For the equatorial phenyl conformation, only two interactions exist between ortho phenyl protons and piperidine axial protons. These provide a 2.7 kcal/mol increase to give a 2.5 kcal/mol net change in nonvicinal van der Waals energy.

MM2 predicts hindered piperidine rotation for PAP, with the conformation determined by X-ray crystallography for the solid preferred. This is separated by a 15.9 kcal/mol barrier from a second local minima, which is 10.2 kcal/mol above the global minimum. This local minimum is midway between the next staggered and *cis*-phenyl/lone pair eclipsed geometry.

For phenyl-axial PCP, piperidine rotation shows nearly an ideal threefold potential, with the two staggered minima lying 0.6 kcal/mol above the global minimum; these are separated by barriers of 6.0–6.5 kcal/mol. For piperidine-axial PCP, the results are intermediate, with barriers of 10.0–10.2 and a local minimum at 5.4 kcal/mol.

These results suggest that piperidine rotation should be rapid on the NMR time scale for PCP, particularly if activation barriers are exaggerated. Thus, spectra are average positions of three rapidly equilibrating conformers.

(16) Burkert, U.; Allinger, N. L. *J. Comput. Chem.* **1982**, *3*, 40.

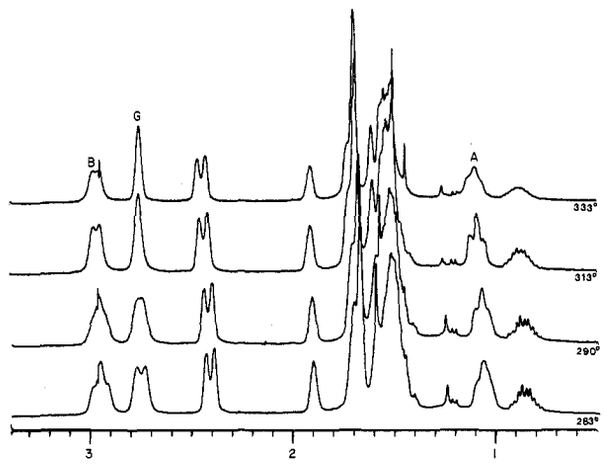

Figure 8. High-field portion of ^1H NMR spectra of NPAP at various temperatures.

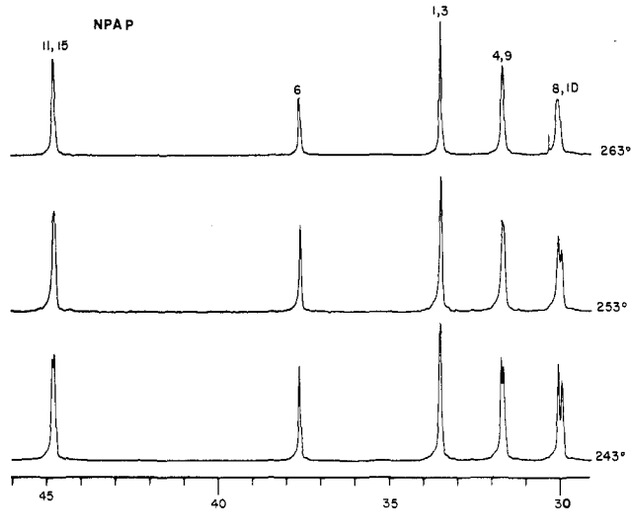

Figure 9. High-field portion of ^{13}C NMR spectra of NPAP at various temperatures. Resonances are labeled according to the numbering scheme in Figure 5.

On the other hand, piperidine rotation or inversion may be observable experimentally in PAP.

Variable-Temperature NMR Studies. Both proton and ^{13}C NMR spectra of PAP were recorded at various temperatures in order to determine the energy required for rotation about the phenyl–adamantyl bond. Variable-temperature proton NMR spectra of PCP, PAP, their *m*-nitro derivatives, and their hydrochloride salts were also recorded in order to determine the phenyl–cyclohexyl rotational barrier and those of other conformational processes. Proton spectra were recorded in $CDCl_3$ in 10 °C intervals in the range –60 to +25 °C and at 5 °C intervals around the coalescence temperature. For PCP, spectra were recorded at 5 °C intervals throughout this range.

The phenyl rotational barrier was measurable in NPAP by both ^1H and ^{13}C NMR. In the proton spectrum, at –50 °C, resonances due to protons G appear as two peaks separated by 12.9 Hz. These peaks coalesce at 17 °C, as shown in Figure 8. When the Eyring equation is used, $\Delta G^{\ddagger}_c = (4.575 \times 10^3)T_c(10.319 + \log T_c/K_c)$, where $K_c = \pi\Delta\nu/2^{1/2}$, an activation energy of 15.0 kcal/mol is obtained for this process at coalescence. At low temperature there are also changes in signals due to protons labeled A and B and the strongly overlapping resonances due to C, D, H and J, but these never become sufficiently distinct to be used for independent calculations of activation energies. All of these signals are due to protons in the immediate vicinity of the *m*-nitrophenyl group, so it is reasonable that the conformational process being measured is phenyl rotation. Variable-temperature spectra of both NPCP and NPCP·HCl again show changes in the corresponding signals but are indistinct, perhaps due to a lower energy barrier for this process. In the ^{13}C NMR spectrum of NPAP (Figure 9), there are also changes at different temperatures that can be used for determination of the phenyl rotational barrier. The signals due to carbons 8 and 10 split into two signals separated by 9.8 Hz at –50 °C and coalesce at –10 °C, indicating a conformational barrier of 13.7 kcal/mol. Signals due to carbons 4 and 9 as well as 11 and 15 (4.9-Hz separation at –50 °C) coalesce at –20 °C, indicating an activation energy of 13.5 kcal/mol. On the basis of ^1H and ^{13}C variable-temperature NMR results, we conclude that the energy of phenyl rotation is 13–15 kcal/mol for the adamantyl derivatives and less for the phencyclidines. The discrepancy in the activation free energy barriers measured in the ^1H and ^{13}C NMR spectra are indicative of the types of errors expected in such coalescence measurements. The barriers measured in this way are expected to be accurate to ±10%.

Variable-temperature ^1H NMR spectra for free bases, PCP and NPCP, show drastic changes, while rigid analogue and hydrochloride salt spectra are relatively unperturbed by temperature variations. Conformational processes that interchange axial and equatorial protons on both the piperidine and cyclohexyl moiety are indicated. Piperidine axial and equatorial protons α to nitrogen are separated by about 500 Hz at –60 °C and coalesce at –5 °C for carbon 5. This leads to an activation energy of 11.9 kcal/mol for exchange of the piperidine protons. Similarly, in the *m*-nitro derivative, NPCP, these peaks are separated by 488 Hz at low temperature and coalesce at –15 °C, leading to an activation energy of 11.4 kcal/mol for nitrogen rotation–inversion barrier.

Thus, barriers of 11–12 kcal/mol are found for interconversion of axial and equatorial protons for both halves of the molecule. It is possible that the processes interchanging axial and equatorial protons are correlated, since their activation energies are similar. Since these processes are absent in the protonated form, they depend on nitrogen inversion. The only path that would result in exchange of axial and equatorial protons is nitrogen inversion, followed or accompanied by 180° rotation of the piperidine ring. We cannot determine experimentally which of these has the higher barrier.

Conclusion

The preferred conformation for PCP and its rigid analogues in solution is identical with its solid conformation, but in the free base there exist other low energy conformations accessible by cyclohexyl ring inversion and piperidine rotation. The nitrogen inversion–rotation barrier is estimated to be 11–12 kcal/mol. A similar barrier, 13–15 kcal/mol, exists for phenyl rotation. This barrier is probably lower in PCP itself, since the more flexible cyclohexyl ring flattens and can more easily distort to relieve interactions between phenyl ortho hydrogens and the C3 and C5 axial hydrogens in the transition state for phenyl rotation. Superimposed on this may be a piperidine rotation process favoring staggered conformations about the piperidine–cyclohexyl bond, not observed in the rigid analogues. However PAP is likely to complex with receptors in its minimum energy conformation with respect to phenyl rotation because higher energy conformations will not be significantly populated at room temperature. Since PCP and PAP have similar pharmacological properties at muscarinic cholinegic receptors, we propose that

the conformations shown in Figure 7 are the only reasonable binding conformations of PCP and acetylcholine. Only the rotation of the piperidine ring differs from that proposed in Figure 1.[2]

Acknowledgment. We are grateful for the insights and encouragement provided by H. Weinstein, R. Osman, B. Pazhenchevsky, and S. Maayani of the Mt. Sinai School of Medicine, to an anonymous referee for incisive comments on the interesting features of the PAP crystal structure, to the National Institute on Drug Abuse for financial support of this research (KNH), and to the National Science Foundation whose support made the acquisition of the 300-MHz NMR spectrometer (University of Pittsburgh) and X-ray diffractometer (Louisiana State University) possible. The 600-MHz NMR spectrum was obtained at the National Institutes of Health facility operated by the Carnegie-Pittsburgh-Mellon Corp.

Registry No. PAP, 72241-99-7; PAP·HCl, 84279-47-0; NPAP, 84279-48-1; NPAP·HCl, 84279-49-2; PCP, 77-10-1; PCP·HCl, 956-90-1; NPCP, 70227-29-1; NPCP·HCl, 84279-50-5.

Supplementary Material Available: X-ray structure factors for PAP (7 pages). Ordering information is given on any current masthead page.

The Antihypertensive and Positive Inotropic Diterpene Forskolin: Effects of Structural Modifications on Its Activity

Sujata V. Bhat, Alihussein N. Dohadwalla, Balbir S. Bajwa, Nandkumar K. Dadkar, Horst Dornauer, and Noel J. de Souza*

Research Centre, Hoechst Pharmaceuticals Limited, Bombay 400 080, India. *Received September 8, 1982*

Four naturally occurring analogues of forskolin were isolated. Forty-nine semisynthetic derivatives were prepared, incorporating structural alterations at the 1-, 6-, 7-, 9-, 11-, and 14/15-positions. Blood pressure lowering properties of 53 compounds were assessed in anesthetized normotensive cats and of 31 compounds in conscious spontaneously hypertensive (SH) rats. The positive inotropic properties of 25 compounds were investigated in an isolated guinea pig atrial preparation. Forskolin was unique among the compounds in its hypotensive activity in cats and in its positive inotropic properties. Although several derivatives displayed oral antihypertensive activity in the SH rats, none was significantly more potent than forskolin. The optimal structural requirements for activity are apparent, since they are found in forskolin itself.

In a program of screening of plants for biological activity, the Indian plant *Coleus forskohlii* Briq. was selected for study of its cardiovascular properties on the basis of its phylogenetic relationship to herbal drugs used in Ayurvedic medicine. Extracts of the roots displayed blood pressure lowering activity in laboratory animals. The major active principle was identified as 7β-acetoxy-8,13-epoxy-1α,6β,9α-trihydroxylabd-14-en-11-one (1), which we named forskolin.[1,2]

The biological profile of the compound and its biochemical properties were unravelled through diverse studies at different laboratories in the following chronological sequence. Forskolin displayed blood pressure lowering properties in normotensive and hypertensive laboratory animals, whether administered intravenously or orally. It also had potent, positive inotropic action and a vasodilatory effect. Its mode of action as an antihypertensive agent was related essentially to its peripheral vasodilatory properties.[3] In biochemical studies, forskolin was found to be an activator of adenylate cyclase.[4]

The unusual structural features and biological profile of this natural product provided the impetus to investigate whether it could be transformed into a more potent antihypertensive or cardioactive molecule with a longer duration of activity, especially when administered orally. One approach undertaken in attempts to attain this objective was a study of the manner in which structural modifications of forskolin would affect its biological profile. This study forms the subject of the current paper as described below. Subsequently, forskolin was shown to be unique in its activation of adenylate cyclase, since activation did not require the guanine nucleotide regulatory protein.[5-7] The mode of positive inotropic action of forskolin was postulated to be due to its activation of cardiac adenylate cyclase via an enhanced calcium uptake by the heart muscle cell.[8] The preclinical pharmacological and toxicological data on forskolin were found to be favorable.[9] Forskolin is now scheduled to undergo trials in human volunteers.

In this report we describe the isolation of naturally occurring forskolin analogues, the synthesis of forskolin derivatives, and a comparison of their antihypertensive and positive inotropic properties relative to forskolin.

Chemistry. The compounds listed in Table I are derivatives of forskolin at the 1α-OH, 6β-OH, 7β-OAc, 9α-OH, 11-(>C=O), and $\Delta^{14,15}$ positions. The compounds are so grouped downwards through the table to reflect the sequential progression from single to multiple alterations at the different positions. Compounds 1, 10, 33, and 37

(1) S. V. Bhat, B. S. Bajwa, H. Dornauer, N. J. de Souza, and H.-W. Fehlhaber, *Tetrahedron Lett.*, 1669 (1977).
(2) V. Shah, S. V. Bhat, B. S. Bajwa, H. Dornauer, and N. J. de Souza, *Planta Med.*, **39**, 183 (1980).
(3) E. Lindner, A. N. Dohadwalla, and B. K. Bhattacharya, *Arzneim.-Forsch.*, **28**, 284 (1976).
(4) H. Metzger and E. Lindner, *IRCS Med. Sci.: Libr. Compend.*, **9**, 99 (1981).
(5) K. B. Seamon, W. Padgett, and J. W. Daly, *Proc. Natl. Acad. Sci. U.S.A.*, **78**, 3363 (1981).
(6) K. B. Seamon and J. W. Daly, *J. Biol. Chem.*, **256**, 9799 (1981).
(7) J. W. Daly, W. Padgett, and K. B. Seamon, *J. Neurochem.*, **38**, 532 (1982).
(8) H. Metzger and E. Lindner, *Arzneim.-Forsch.*, **31**, 1248 (1981).
(9) Preclinical studies were completed at the authors' laboratories and those of Hoechst AG., Frankfurt, in preparation for the filing of an IND application.

0022-2623/83/1826-0486$01.50/0